6. Impedance and Beam Instabilities in Synchrotron Light Sources

高エネルギー加速器研究機構 Tanaka Olga

### 目 次

### Impedance and Beam Instabilities in Synchrotron Light Sources

1.	Introduction: Historical Overview	<b>6</b> – 1
2.	Introduction to Wake Fields and Impedance	<b>6</b> – 2
	2.1 Time-Domain Wake Function	<b>6</b> – 2
	2.2 Frequency-Domain Impedance	<b>6</b> – 3
3.	Modeling Impedance of Structures ·····	
	3.1 RF Cavity Impedance ·····	
	3.2 Resistive-Wall Impedance ·····	
	3.3 Geometric Discontinuities and Step Transitions	
	3.4 Cross-Sectional Effects: Elliptical and Racetrack Pipes	
	3.5 Numerical Methods for Geometrical Impedance	
	3.6 Major Impedance Contributors in Synchrotron Light Sources	<b>6</b> – 9
	3.7 Impedance budgeting ·····	<b>6</b> – 9
4.	Beam Dynamics under the Influence of Impedance	
	4.1 Longitudinal Impedance and Energy Loss	
	4.2 Longitudinal Potential Well Distortion	
	4.3 Longitudinal Coupled-Bunch Tune Shifts	
	4.4 Transverse Impedance and Tune Shifts	
	4.5 Instability Thresholds	<b>6</b> −11
5.	Introduction to Beam Instabilities	
	5.1 Classification of Instabilities ·····	
	5.2 Head-Tail Instability ·····	
	5.3 Coupled-Bunch Instabilities	
	5.4 Transverse Mode Coupling Instability (TMCI)	
	5.5 Growth Rates and Damping Mechanisms	
	5.6 Summary of Stability Criteria	<b>6</b> −13
6.	Summary ·····	<b>6</b> −13
7	References	6-13

### Impedance and Beam Instabilities in Synchrotron Light Sources

### 1. Introduction: Historical Overview

As synchrotron light sources have advanced toward higher beam currents and lower emittances, collective effects – arising from electromagnetic interactions between the beam and surrounding structures – have become increasingly critical to beam stability and performance. These interactions are described in the **time domain** by *wake fields*, and in the **frequency domain** by their Fourier transforms, known as *beam coupling impedances*.

The theoretical foundation for these concepts was laid in the mid-20th century. One of the earliest rigorous treatments of wake fields appeared in the seminal work by W.K.H. Panofsky and W.A. Wenzel [1], which described how charged particles induce electromagnetic fields in accelerator structures. The notion of impedance as a tool to quantify such interactions was first introduced at CERN in the 1960s. V.G. Vaccaro's internal ISR reports (1966) [2] articulated the longitudinal stability conditions for coasting beams in terms of coupling impedance.

A landmark development followed with **E. Keil and W.D. Schnell**'s proposal of the **Keil–Schnell criterion** [3], providing a stability condition that relates longitudinal impedance to the beam's momentum spread. This work formalized the idea that excessive impedance can lead to beam instabilities, and it became a cornerstone in collective beam dynamics.

Further theoretical advancement came with **A.W. Chao**'s 1980 Ph.D. thesis and his authoritative book *Physics of Collective Beam Instabilities in High Energy Accelerators* [4]. Chao's work provided a unified and systematic treatment of both longitudinal and transverse instabilities, clarifying the connection between wake functions, impedance spectra, and instability thresholds across various accelerator regimes.

In parallel, **T. Weiland** [5] developed advanced time-domain numerical methods to compute wake potentials in realistic accelerator structures, a major step toward practical wake field simulations. At **SLAC**, researchers such as **K.L.F. Bane** and **M. Sands** [6]

contributed foundational results on short-bunch wake fields in RF cavities. Meanwhile, at CERN, F. J. Sacherer [7] established key stability formalisms, and K. Yokoya later extended impedance theory to include non-cylindrical geometries and resistive-wall effects [8], [9].

Historically, impedance evaluations at the Photon Factory (PF) relied on both direct measurement techniques and operational diagnostics, substantial contributions from a core group of researchers. In the late 1980s and early 1990s, M. Izawa, H. Kobayakawa, and S. Sakanaka played a central role in investigating beam instabilities caused by higher-order modes in accelerating cavities, leading to effective damping strategies and coupler designs (see [10], [11]). Their work culminated in pioneering impedance measurement experiments at PF, integrating advanced diagnostics with machine studies [12]. S. Sakanaka further advanced impedance characterization through precise observation of quadrupolar tune shifts after PF ring upgrades, linking these shifts to impedance sources and validating them with beambased measurements [13], [14]. N. Nakamura and collaborators also contributed to understanding collective effects in single-bunch operation, highlighting PF's role as a testbed for instability suppression techniques [15].

The OHO seminar series has systematically built a deep and coherent understanding of wake fields and impedance effects over time. Notably, **Y.H. Chin's seminal lectures in 1996 and 1999** provided the theoretical backbone for many subsequent studies and formed the basis for practical impedance evaluation methods now used at KEK and other facilities [16], [17]. Later lectures by **Y. Shobuda** (2011), further developed this knowledge, integrating it with simulation techniques, and analytical evaluations [18].

The present lecture builds upon these foundational studies and aims to reflect recent advancements in impedance modeling and control, with a particular focus on modern impedance budgeting strategies for high-brightness and ultralow emittance synchrotron light sources. It revisits classical concepts through the lens of current design challenges and mitigation techniques in next-generation storage rings.

# 2. Introduction to Wake Fields and Impedance

When a charged particle bunch traverses a vacuum chamber or RF structure in an accelerator, it excites electromagnetic fields due to its interaction with the surrounding conducting surfaces and discontinuities. These fields persist after the particle passes and can act on subsequent particles in the bunch or in following bunches. This interaction is known as the **wake field** [16] - [18].

The wake field is the electromagnetic field generated by a charged particle as it moves through an accelerator structure, which acts back on other particles that follow it along the beam path.

• The particle that generates the wake is called the **source particle**.

A source particle is a beam particle (or a bunch of particles) that passes through an accelerator element first, exciting wake fields that may influence subsequent particles.

• Particles affected by the wake fields are referred to as **test particles**.

Test particles are beam particles that follow the source particle and experience the wake field left behind, leading to changes in energy (longitudinal effect) or trajectory (transverse effect).

Depending on the nature of the field and its orientation relative to the beam direction, the wake field can be categorized into:

- The longitudinal wake field, which affects the energy gain or loss of trailing particles.
- The transverse wake field, which imparts a deflection or focusing effect in the transverse direction.

To analyze beam-environment interactions more conveniently, we use the **beam coupling impedance**  $Z(\omega)$ , which is the frequency-domain representation of the wake field and acts as a transfer function from beam current to induced voltage [4]:

$$V(\omega) = Z(\omega)I(\omega) \tag{2-1}$$

The beam coupling impedance quantifies how the accelerator structure responds to beam current oscillations at different frequencies. It determines how much voltage is induced by a given current modulation.

#### 2.1. Time-Domain Wake Function

The **wake function** provides a quantitative description of the effect of a source particle on a test particle. It is defined as the voltage (longitudinal) or transverse kick (transverse) experienced by a test particle at a distance s behind the leading one.

The wake function characterizes the field left behind by a moving charge, evaluated at the location of a test particle. It captures the space-time dependence of beam-induced forces and is a key tool in modeling collective effects.

• The **longitudinal wake function** W||(s) gives the energy change per unit charge of the test particle:

$$W_{\parallel}(s) = -\frac{1}{q} \int E_z(z, t) dz$$
for  $s > 0$  (2-2)

 The transverse wake function W<sub>⊥</sub>(s) gives the transverse momentum kick per unit charge and per unit displacement of the source particle.

Important physical features of wake functions include:

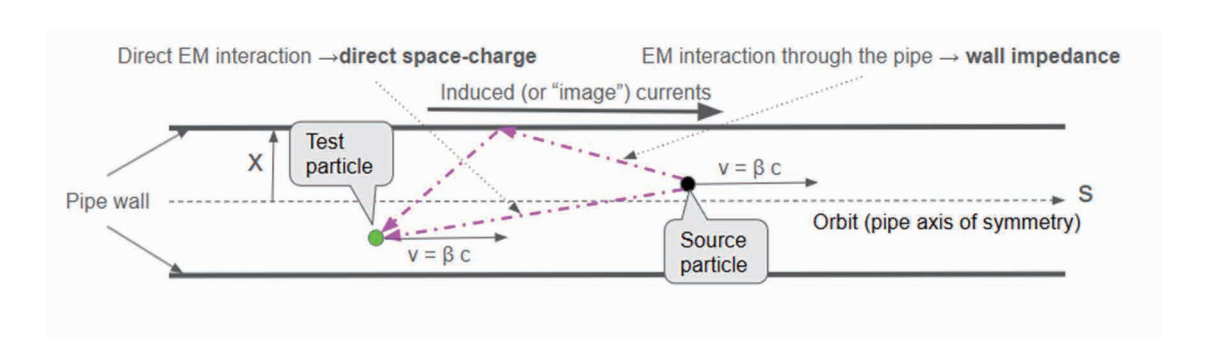


Fig. 1 Generation of wake fields due to image currents.

• Causality: The wake field cannot act backward in time, so W(s)=0 for s < 0.

Causality ensures that only test particles are influenced, reflecting the physical limit of electromagnetic field propagation.

- Short-range vs long-range wakes: Short-range wake functions decay rapidly with distance s and are important for single-bunch effects such as intra-bunch energy spread and transverse mode coupling. Long-range wakes, which persist over many RF buckets or revolutions, drive multibunch (coupled-bunch) instabilities.
- **Decay behavior**: For a resistive wall, the wake function decays approximately as ∝1/√s [6]; for cavities, the wake may oscillate and decay slowly depending on the quality factor Q.

### 2.2. Frequency-Domain Impedance

By applying a Fourier transform to the wake function, we obtain the **impedance**  $Z(\omega)$ , which describes how the induced voltage responds to beam current oscillations at different frequencies:

$$Z_{\parallel}(\omega) = \int_{0}^{\infty} W_{\parallel}(s) e^{\frac{i\omega s}{c}} ds,$$

$$Z_{\perp}(\omega) = \frac{i}{c} \int_{0}^{\infty} W_{\perp}(s) e^{\frac{i\omega s}{c}} ds.$$
(2-3)

The Fourier transform is a mathematical operation that converts a time- or space-domain signal into its frequency components. It reveals the resonant and reactive characteristics of the beam - structure interaction.

The impedance possesses several mathematical and physical properties:

- Causality and analyticity: Because wake functions are causal, their Fourier transforms (impedances) are analytic functions in the upper half of the complex plane, satisfying Kramers Kronig relations.
- **Symmetry**: For real wake functions,  $Z(-\omega)^* = Z(\omega)$ .
- Panofsky-Wenzel theorem [1]: This fundamental relation links longitudinal and transverse impedance:

$$\vec{\nabla}_{\perp} Z_{\parallel} = i\omega Z_{\perp}$$

The Panofsky-Wenzel theorem expresses that the transverse impedance can be derived from spatial derivatives of the longitudinal impedance, under the assumption of slowly varying fields and linear beam dynamics.

In practice, impedance spectra can be classified into:

• **Broadband impedance**: Smooth, low-Q contributions arising from resistive walls, surface roughness, and chamber transitions. They affect single-bunch stability and energy loss.

Broadband impedance is typically modeled by effective RLC circuits with wide frequency response and is responsible for phenomena like turbulent bunch lengthening.

 Narrowband impedance: Sharp resonances due to higher-order modes in RF cavities or trapped modes in chamber discontinuities. They are the main drivers of coupled-bunch instabilities.

Narrowband impedance corresponds to localized resonances that strongly affect specific frequency components, often requiring damping or detuning to mitigate instabilities.

Understanding the impedance spectrum of a storage ring is essential for accurate predictions of energy loss, tune shifts, and instability thresholds. Impedance budgeting and beam-based measurements are standard tools at modern facilities [4], [8].

### 3. Modeling Impedance of Structures

In synchrotron light sources, several key components contribute significantly to the overall beam coupling impedance, affecting energy loss, bunch shape, and beam stability. Among the most critical are insertion devices (IDs) such as in-vacuum undulators and wigglers, which often have narrow gaps and tapered transitions, leading to strong resistive-wall and geometrical impedance. RF cavities are another major source, contributing narrowband impedance through high-Q resonant modes that can drive coupledbunch instabilities unless effectively damped. Beam position monitors (BPMs), with their discontinuous electrode geometry, add high-frequency geometrical impedance, while bellows and flanges – necessary for mechanical flexibility - act like small cavities unless shielded, contributing to broadband impedance. Transitions and tapers between different vacuum

chamber sections introduce significant geometrical impedance if not smoothly designed, especially in narrow-aperture regions. The **resistive-wall impedance** arises from the finite conductivity of vacuum chamber materials and is dominant over long sections such as straight beamlines and insertion regions. Additional sources include **diagnostic and injection devices** (e.g., kickers, septa, and screens), which often have complex geometries; **surface** 

roughness and coatings, which enhance high-frequency impedance; and collimators or scrapers, which, due to their proximity to the beam, contribute substantial transverse impedance. Effective impedance control requires careful design, shielding, and material selection across all these components. Let us discuss in details the three major ring impedance contributors: RF cavities, resistive-wall, and geometrical impedances.







Fig. 2 Examples of impedance contributors at storage rings: a). Taper between the flange and the undulator for the geometrical impedance; b). Copper plate on top of the undulator for the resistive-wall impedance; c). Step transition from the octagon to the rectangular chambers.

### 3.1. RF Cavity Impedance

In storage rings and linear accelerators, **RF cavities** serve as the primary source of acceleration. However, beyond their intended accelerating mode, cavities inherently support **higher-order modes (HOMs)** that persist after the bunch passage and can interfere with subsequent bunches. These fields give rise to **cavity impedance**, a major source of both *narrowband* and *broadband* impedance that affects beam stability.

The *cavity impedance* refers to the component of the beam coupling impedance arising from the interaction of the beam with resonant electromagnetic modes supported by an RF cavity. It is often dominated by *higher-order modes* (HOMs) — electromagnetic eigenmodes other than the fundamental accelerating mode — which can store energy and reinteract with trailing bunches.

Cavity impedance can be decomposed into:

- Longitudinal cavity impedance, which affects the energy distribution within the bunch and can lead to bunch lengthening or microwave instabilities.
- Transverse cavity impedance, which can drive coupled-bunch or head-tail instabilities, particularly for modes with non-zero transverse electric fields.

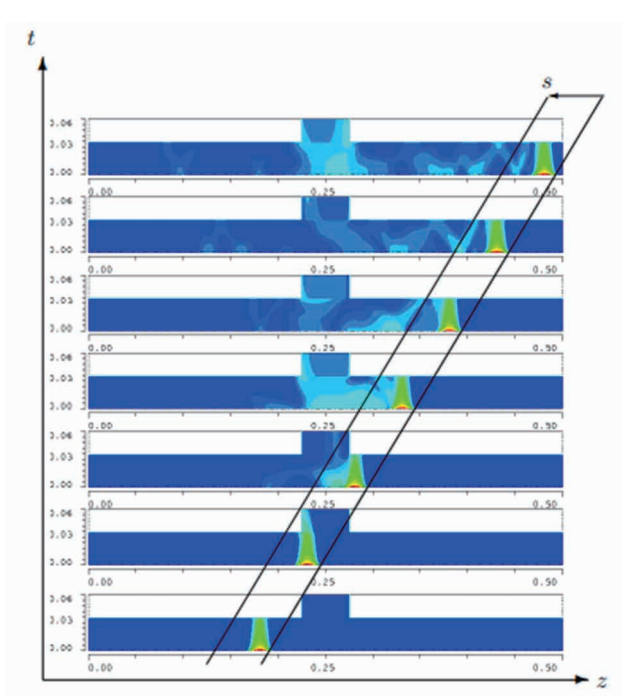


Fig. 3 Wake fields generated by a Gaussian bunch traversing a cavity (taken from Fig. 5 in Ref. [19]).

The *cavity impedance* refers to the component of the beam coupling impedance arising from the interaction of the beam with resonant electromagnetic modes supported by an RF cavity. It is often dominated by *higher-order modes* (HOMs) – electromagnetic eigenmodes other than the fundamental accelerating

mode – which can store energy and reinteract with trailing bunches.

Cavity impedance can be decomposed into:

- Longitudinal cavity impedance, which affects the energy distribution within the bunch and can lead to bunch lengthening or microwave instabilities.
- Transverse cavity impedance, which can drive coupled-bunch or head-tail instabilities, particularly for modes with non-zero transverse electric fields.

#### 3.1.1. Impedance of a Resonant Mode

A widely used approach for modeling impedance from resonant structures is the RLC resonator model [4], [20]. In this model, a given mode is represented by a parallel (or series) resistor-inductor-capacitor (RLC) circuit, which exhibits a resonance at its natural frequency.

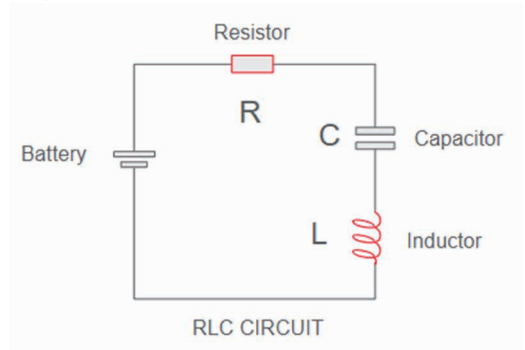


Fig. 4 Cavity resonator and equivalent circuit: RLC parallel resonant circuit.

An RLC circuit is an idealized electrical circuit composed of resistance R, inductance L, and capacitance C. It captures the frequency-dependent behavior of resonant electromagnetic modes in cavity-like structures.

The longitudinal impedance of such a mode is given by:

$$Z_{\parallel}(\omega) = \frac{R_s}{1 + iQ\left(\frac{\omega}{\omega_r} - \frac{\omega_r}{\omega}\right)},$$
(3-1)

where:

- R<sub>s</sub>: Shunt impedance, which characterizes how effectively a given mode converts beam power into voltage.
- $\omega_r$ : *Resonant frequency* of the mode.

• Q: Quality factor, a dimensionless parameter that describes how underdamped the resonance is.

The shunt impedance  $R_s$  measures the voltage developed across a resonator per unit power dissipated. Higher values of  $R_s$  indicate more significant beam-cavity interaction.

The resonant frequency  $\omega_r$  is the natural oscillation frequency of the mode and determines where in the frequency spectrum the impedance peak appears.

The quality factor Q is defined as  $Q = \omega_r L/R$  or equivalently  $Q = \omega_r/\Delta\omega$ , where  $\Delta\omega$  is the full-width at half-maximum of the impedance peak. High-Q resonators store energy for a long time and contribute to long-range wake fields.

In modern light sources, radio-frequency (RF) cavities — which are structures used to accelerate and maintain the energy of particle beams using electromagnetic fields — are often operated in continuous wave (CW) or high-repetition modes, where multi-bunch effects dominate. Even weak higher-order modes (HOMs) can drive longitudinal coupled-bunch instabilities unless adequately damped. Thus, cavity impedance characterization is central to:

- HOM damping system design,
- Coupled-bunch feedback systems,
- Accurate impedance budgeting.

Furthermore, as synchrotron light sources push toward **shorter bunches** and **higher currents**, the **transverse impedance** from cavity asymmetries becomes increasingly critical [21].

#### 3.2. Resistive-Wall Impedance

In many accelerator components, such as flat vacuum chambers, dechirpers, and certain beam collimators, the beam traverses a structure that can be approximated as two **infinite parallel conducting plates**. When these plates have *finite electrical conductivity*, they give rise to **resistive-wall impedance**, which influences the longitudinal and transverse stability of the beam.

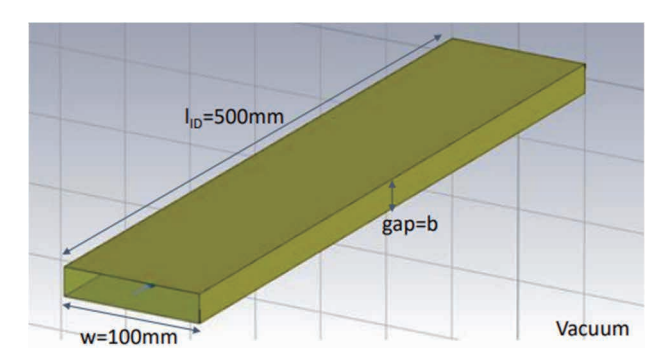


Fig. 5 CST model of the undulator RF shielded by the copper sheet.

When a relativistic charged particle bunch passes between two conductive plates, it induces *image currents* on the surfaces. If the plates have *finite conductivity*  $\sigma$ , the image currents experience Ohmic losses. These losses generate electromagnetic fields that **linger** and act back on trailing particles – this is the source of the **resistive-wall wake field**.

The Fourier transform of this wake field gives the **resistive-wall impedance**, which in the case of parallel plates can differ significantly from that of a circular or elliptical pipe due to the geometry of the field lines and current paths.

Consider two infinite, perfectly flat metal plates separated by a distance 2b, where b is the half-gap between the plates. A beam moves in the longitudinal direction (z-axis) between the plates, centered at y=0. The plates are assumed to be:

- infinitely wide in the transverse x-direction,
- thickness of the plates, is negligible,
- composed of a material with conductivity  $\sigma$  and relative permeability  $\mu_r \approx 1$ .

The impedance calculation assumes the skin depth is small compared to the plate thickness (valid at high frequency), and that the beam's transverse size is much smaller than the gap.

The *longitudinal resistive-wall impedance per unit length* between parallel plates is given, in the frequency domain, by the following expression [22], [23]:

A widely used model for the **longitudinal resistive**wall impedance of a circular beam pipe with radius b and wall conductivity  $\sigma$  is:

$$Z_{\parallel}^{plates}(\omega) = (i+1)\frac{Z_0}{2\pi b}\sqrt{\frac{\omega}{2\sigma}},$$
 (3-2)

where:

- $Z_0 = \sqrt{\mu_0/\varepsilon_0} \approx 377 \ \Omega$  is the vacuum impedance,
- *b* is the half-gap between the plates,
- σ is the conductivity of the material (e.g., copper, stainless steel),
- ω is the angular frequency of the beam-induced fields.

This impedance increases with frequency as  $\sqrt{\omega}$ , decreases with the square root of the conductivity, inversely scales with the half-gap b. The **real part** corresponds to resistive energy loss (heating), while the **imaginary part** contributes to collective effects such as **bunch lengthening** and **potential well distortion**.

The corresponding expression for the **transverse resistive-wall impedance per unit length**, relevant for driving transverse instabilities, is [24]:

$$Z_{\perp}^{plates}(\omega) = (i+1)\frac{cZ_0}{2\pi b^3} \sqrt{\frac{1}{2\sigma\omega}},$$
(3-3)

where c is the speed of light. Notably,  $Z_{\perp}$  decreases with frequency as  $1/\sqrt{\omega}$ , and increases strongly as  $1/b^3$ , making narrow-aperture chambers especially problematic for transverse beam stability. The transverse impedance governs the strength of dipolar wake fields, which can lead to beam breakup, head-tail, and coupled-bunch instabilities.

These resistive-wall impedances are **long-range**, meaning their wake fields persist over distances longer than the bunch length and can drive **multi-bunch instabilities** if not properly controlled. This component can drive **transverse mode coupling instability** (TMCI) or **coupled-bunch instabilities**, particularly dangerous at high beam currents.

Materials such as **aluminum**, **copper**, and **stainless steel** offer trade-offs between conductivity and mechanical or vacuum properties. Coatings like **TiN**, **NEG**, or **amorphous carbon** can also affect impedance, especially at very high frequencies (THz range), relevant for short bunches.

The conductivity  $\sigma$  of a material indicates its ability to carry current. High-conductivity materials (e.g., copper) reduce resistive impedance, while lower-conductivity materials increase energy loss and instability risks.

### 3.3. Geometric Discontinuities and Step Transitions

Discontinuities in the beam pipe – such as bellows, vacuum flanges, kickers, and beam position monitors (BPMs) – create abrupt changes in geometry, generating localized wake fields.

Geometric discontinuities are changes in the crosssection or topology of the vacuum chamber that interrupt the smooth flow of electromagnetic fields, causing reflection, trapping, and radiation of wake fields.

Examples include:

- Step transitions: sudden changes in pipe radius.
- **Tapers**: gradual changes used to minimize wake excitation.
- Bellows: flexible sections that accommodate alignment changes but can introduce high impedance unless shielded.

For a sudden step in radius from a to b, the longitudinal wake potential exhibits a delta-like

structure, while the impedance increases significantly for high frequencies unless smoothed with tapers or RF shields.

It reflects how these structures deflect or retard the beam-induced electromagnetic fields, thereby producing *wake fields* that feed back onto the beam. Importantly, it is **purely geometrical**, meaning it exists even for a perfectly conducting wall  $(\sigma \rightarrow \infty)$  [25], [26], [27].

Key features of the geometrical impedance are the following. Geometrical impedance is **dominant at low frequencies** and for **ultra-relativistic beams**, it often dictates the **broadband** component of the impedance budget. Unlike resistive-wall impedance, it **does not vanish** in the limit of zero material loss. It can cause **significant energy loss**, **bunch deformation**, and **transverse kicks**, especially in small-aperture regions like insertion devices or collimator tapers.

Design strategies include:

 RF shielding of bellows with sliding fingers or convoluted shields.

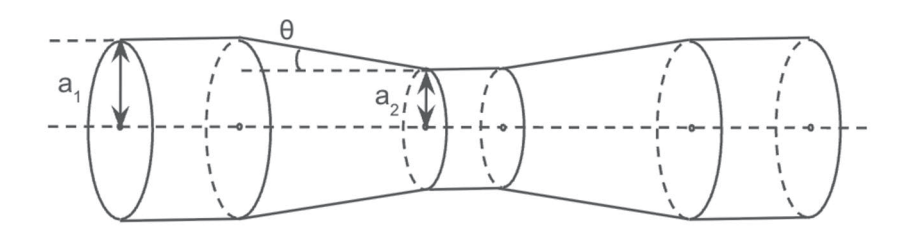


Fig. 6 The geometrical structure of tapered transitions.

- Adiabatic tapers, which minimize reflection and reduce broadband impedance.
- Matching cross-sectional geometries to maintain beam symmetry.

### 3.4. Cross-Sectional Effects: Elliptical and Racetrack Pipes

In light sources, vacuum chambers are often non-circular – **elliptical**, **racetrack**, or **rectangular** – to allow for photon beam extraction. These shapes break axial symmetry and complicate impedance calculations.

Elliptical beam pipes have differing horizontal and vertical radii, which can affect field patterns, impedance, and resonance modes. Racetrack cross-

sections combine flat sections with rounded corners, commonly used in magnet gaps.

These shapes can:

- Alter mode cutoff frequencies.
- Enhance **trapped modes** in certain locations (e.g., RF-shielded flanges).
- Increase **transverse impedance anisotropy** between horizontal and vertical planes.

Simulation tools or analytical methods based on conformal mapping are used to estimate impedance in such geometries [12].

## 3.5. Numerical Methods for Geometrical Impedance

Analytical models are limited to simple geometries. For realistic, complex components (e.g., LHC collimators or undulator transitions), **numerical electromagnetic solvers** are used.

### 3.5.1. Time-Domain Solvers

These simulate the passage of a charged bunch through a structure and compute wake potentials as a function of time or distance behind the bunch (Table 1).

### 3.5.2. Frequency-Domain Solvers

These solve Maxwell's equations at fixed frequencies and are suited for high-Q resonant structures or mode identification (Table 2).

Table 1 Time domain solvers

Code	Description	Reference or Developer	
CST Particle Studio	Commercial 3D electromagnetic PIC solver for	CST Studio Suite, Dassault	
(Wakefield Solver)	wake potential calculation.	Systèmes, [28].	
GdfidL	Finite-Difference Time-Domain (FDTD) solver	I Zaganadnay at al. [20]	
GulluL	tailored for wakefield and impedance problems.	I. Zagorodnov et al., [29].	
ECHO / ECHO2D	Time-domain code for wakefield calculation in	H. Zagorodnov, T. Weiland,	
ECHO/ECHO2D	axisymmetric structures.	[30].	
OpenEMS	Open-source FDTD-based Maxwell solver,	openEMS Project, [31].	
OpenEMS	adaptable to wakefield analysis.	openewis Project, [31].	
ABCI	2D time-domain code for axially symmetric	Y. H. Chin et al., [32].	
ADCI	structures.		
TBCI	Early time-domain code developed at KEK for	T Wailand at al. [22]	
IDCI	rectangular and cylindrical geometries.	T. Weiland et al., [33].	

**Table 2 Frequency domain solvers** 

Code	Description	Reference or Developer	
HFSS (Ansys)	Finite Element Method (FEM) solver for full 3D structures, widely used for HOM analysis.	Ansys HFSS, [34].	
CST Particle Studio (Frequency Domain Solver)	Part of CST Studio; FEM-based, efficient for eigenmode and S-parameter analysis.	CST Studio Suite, Dassault Systèmes, [28].	
ACE3P	Suite developed at SLAC for large-scale, parallel eigenmode and wakefield simulations.	SLAC National Accelerator Laboratory, [35].	
MAFIA	Early multipurpose 3D frequency-domain solver. Now deprecated.	R. Gluckstern et al., DESY, [36].	
OMEGA3P	Eigenmode solver part of ACE3P used for HOM calculations.	SLAC, [37].	
Superfish	2D eigenmode solver, best for axisymmetric RF cavities.	LANL, [38].	
URMEL / URMEL-T	Frequency-domain code for longitudinal/transverse impedance of RF cavities.	DESY, [39].	

These tools are used to build detailed **impedance databases** for modern machines like the LHC, **SIRIUS**, and **MAX IV** [40], [41], [42].

### 3.6. Major Impedance Contributors in Synchrotron Light Sources

Here is a table summarizing the major impedance contributors in several currently operating synchrotron light sources, including the Photon Factory (PF). It highlights the dominant impedance sources in each machine and typical mitigation strategies (see Table 3).

### 3.7. Impedance budgeting

In modern synchrotron light sources, **impedance budgeting** is a critical process in machine design and beam stability control. An *impedance budget* is the systematic evaluation and summation of all known contributions to the accelerator's total beam coupling impedance, which arises from electromagnetic interactions between the beam and surrounding structures. The *longitudinal impedance* affects energy spread and bunch lengthening, while the *transverse impedance* can drive beam instabilities such as the transverse mode coupling instability (TMCI). Accurate impedance budgeting ensures that the *thresholds for beam instabilities* – such as coupled-bunch growth or microwave instability – remain above nominal operating currents.

To construct this budget, each accelerator component - RF cavities, vacuum chamber discontinuities, bellows, BPMs, in-vacuum undulators, and injection kickers - is modeled or measured, often using numerical methods (e.g., CST, GdfidL) or beam-based techniques. The budget is then benchmarked against known instability theories (e.g., Keil-Schnell criterion, Sacherer formalism) to validate design margins. For example, in the Photon Factory (PF), impedance studies revealed that bellows and geometric transitions contributed significantly to broadband impedance, while HOMs from RF cavities were the primary drivers of longitudinal instabilities [25], [10]. Similarly, facilities like MAX IV and ESRF-EBS employ ultrasmooth chamber designs and HOM-free cavities to suppress impedance sources [43].

A well-maintained impedance budget not only supports beam stability but also guides decisions in upgrades and high-current operations. It is a cornerstone of the impedance control strategy in diffraction-limited storage rings and next-generation light sources.

**Table 3 Major Impedance Contributors in Modern Synchrotron Light Sources** 

Facility	RF Cavities (HOMs)	Vacuum Chamber Geometry	In-Vacuum Undulators	Flanges / BPMs / Bellows	Kickers / Injection Systems	Notable References
Photon Factory (PF)	Significant source of longitudinal CB instabilities	Tapers, transitions (notably PF- AR sections)	Moderate; evaluated in detail	Bellows and BPMs dominant in PF Upgrade	Septum kicker, injection chamber	M. Izawa et al. (1987), [10].
ALS (Berkeley)	HOMs damped in SR cavities	Narrow gaps, tapers in arc sections	Present; moderate impact	Tapers and bellows major contributors	Injection kickers modeled in budget	D. Wang et al. (2021), [44].
MAX IV	HOM-free cavities designed	Smooth geometry with NEG coating	Low; short bunches, long IDs	Extremely reduced via minimization design	Injection kicker shielded	R. Nagaoka et al. (2014), [45].
Soleil	Significant in earlier designs	Transitions between achromats	Moderate	BPMs and bellows	Kickers included in impedance model	R. Nagaoka et al. (2005), [46].

ESRF-EBS	Strongly damped HOMs	Smooth chamber profile optimized for impedance	Low (optimized)	BPMs and absorbers accounted	Fast injection system considered	ESRF impedance budget report (2019), [47].
BESSY II	RF cavities and multi-cell resonators	Flat elliptical vacuum chamber	Considered in upgrade studies	Bellows significant in multi-bunch mode	Septum injection dominant	S Khan et al. (2005), [48].

### 4. Beam Dynamics under the Influence of Impedance

The interaction between beam particles and the vacuum chamber environment, as described by impedance, leads to measurable changes in fundamental beam parameters such as:

- Tune shifts;
- Energy spread;
- Bunch lengthening;
- Instability growth rates.

These effects can often be analyzed within the **rigid-bunch approximation**, where the bunch shape remains fixed while its collective motion evolves under the influence of the impedance (see [4] and [49] for details).

The rigid-bunch approximation assumes that the beam oscillates, without internal distortion of its charge distribution. This simplifies the analysis of instabilities and is particularly useful for estimating thresholds and tune shifts.

### 4.1. Longitudinal Impedance and Energy Loss

When the beam interacts with longitudinal impedance, it loses energy per turn due to resistive wake fields. This manifests as an **energy loss per particle** and affects RF system requirements.

The **energy loss per turn** U due to the longitudinal impedance  $Z_{\parallel}$  is given by:

$$U = \frac{1}{2\pi} \int_{-\infty}^{\infty} |\tilde{I}(\omega)|^2 Re[Z_{\parallel}(\omega)] d\omega. \tag{4-1}$$

This integral represents the total power dissipated by the beam current spectrum  $\tilde{I}(\omega)$  in the resistive (real) part of the impedance. It generalizes Ohm's law to distributed frequency-dependent systems [19], [50].

The energy loss leads to additional demands on the RF system, and if uncompensated, causes **synchrotron frequency shifts** and **bunch lengthening**.

Synchrotron frequency is the oscillation frequency of particles in longitudinal phase space. A shift in this frequency due to impedance is one of the earliest indicators of longitudinal collective effects [51].

### 4.2. Longitudinal Potential Well Distortion

In a more refined model, the beam sees a modified **longitudinal potential well**, which combines the external RF potential with the voltage induced by the beam itself via the impedance:

$$V_{tot}(z) = V_{RF}(z) + V_{wake}(z).$$
(4-2)

Potential well distortion refers to the reshaping of the equilibrium potential seen by beam particles due to self-induced fields. It modifies the bunch shape and energy spread even below instability thresholds.

This leads to **bunch lengthening** and **energy spread increase**, even in stable beams, a phenomenon commonly observed in storage rings with high broadband impedance [4], [49].

### 4.3. Longitudinal Coupled-Bunch Tune Shifts

For a multi-bunch beam, long-range wake fields from high-Q cavity modes can couple the motion of different bunches. The resulting **coupled-bunch modes** have different growth rates and frequency shifts.

Under the rigid-bunch approximation, the complex frequency shift of mode  $\mu$  is:

$$\Delta\omega_{\mu} = \frac{eI_0}{2E_0T} \sum_{p=-\infty}^{\infty} Z_{\parallel} \left(\omega_0(pM+\mu)\right). \tag{4-3}$$

Here:

• μ: Coupled-bunch mode number;

- *M*: Number of bunches;
- *I*<sub>0</sub>: Total beam current;
- $E_0$ : Beam energy;
- *T*<sub>0</sub>: Revolution period;
- $\omega_0$ : Revolution angular frequency.

Coupled-bunch modes describe collective oscillations of multiple bunches, often driven by high-Q impedances such as HOMs. Mode  $\mu$ =0 corresponds to in-phase oscillation;  $\mu$ =M/2 to out-of-phase.

This formalism enables the estimation of **growth** rates and stability thresholds for different modes, crucial in designing feedback systems or HOM dampers [4], [19], and [49].

### 4.4. Transverse Impedance and Tune Shifts

In the transverse plane, the beam interacts with the **transverse impedance**  $Z_{\perp}$ , resulting in tune shifts and possible instabilities.

The transverse coherent tune shift for mode  $\mu$ :

$$\Delta Q_{\mu} = \frac{eI_0\beta}{4\pi E_0} \sum_{p=-\infty}^{\infty} \frac{Z_{\perp}(\omega_0(pM+\mu))}{\omega_0},$$
(4-4)

where  $\beta$  is the beta function at the location of the impedance.

A coherent tune shift is a shift in the oscillation frequency of the beam centroid due to collective forces. It differs from incoherent tune spread caused by nonlinearities or individual particle dynamics.

When the real part of the impedance is negative at the relevant frequency, the mode can grow – leading to **transverse coupled-bunch instabilities**, often requiring active damping or chromaticity control [4], [49].

#### 4.5. Instability Thresholds

Analytical expressions for **instability thresholds** are important for machine design and operation. For broadband longitudinal impedance, the **Keil–Schnell criterion** gives the threshold current:

$$\left|\frac{Z_{\parallel}}{n}\right| < \frac{2\pi\alpha E\delta^2}{eI_0},\tag{4-5}$$

where:

- $n=\omega/\omega_0$ : Harmonic number;
- α: Momentum compaction factor;

• δ: Relative energy spread.

The Keil–Schnell criterion sets a limit on longitudinal impedance to prevent microwave instability in coasting or bunched beams. It is a foundational tool in impedance budgeting [52], [4].

For transverse instability, the **Boussard criterion** and **Sacherer formulas** provide similar expressions for the maximum tolerable impedance or beam current [53], [54].

#### 5. Introduction to Beam Instabilities

In synchrotron light sources, the electromagnetic interaction between the beam and the surrounding environment – described by the impedance – can lead to various forms of **beam instabilities**, particularly at high beam current or low emittance. These instabilities arise when the energy fed back to the beam by its own wake fields grows faster than it is damped by radiation, feedback systems, or natural decoherence [4], [19], [49].

Beam instabilities are collective oscillations of charged particle beams that grow in amplitude over time, due to self-interactions mediated by wake fields and impedance. They can cause emittance blow-up, beam loss, or reduced lifetime.

Instabilities are broadly classified into **longitudinal** and **transverse**, and further into **single-bunch** and **multi-bunch** phenomena.

#### 5.1. Classification of Instabilities

**Longitudinal instabilities** involve fluctuations in particle energy or arrival time. These include:

- **Microwave instability** (single-bunch): due to broadband impedance [52].
- Longitudinal coupled-bunch instability: due to narrowband impedance, especially HOMs.

**Transverse instabilities** involve oscillations of the beam centroid in the transverse plane. Key examples include:

- Transverse mode coupling instability (TMCI): single-bunch phenomenon driven by broadband impedance [54].
- Transverse coupled-bunch instability: typically caused by high-Q modes in RF cavities or kickers [53].

The following subsections provide an introduction to the dominant mechanisms relevant for light sources.

### 5.2. Head-Tail Instability

One of the most fundamental instabilities in bunched beams is the **head-tail instability**, driven by shortrange transverse wake fields and chromatic effects.

The head-tail instability arises when different longitudinal slices of the bunch experience different transverse kicks due to wake fields and phase shifts induced by chromaticity. The "head" of the bunch excites a wake that deflects the "tail."

This instability is characterized by:

- **Mode coupling** between transverse betatron motion and synchrotron oscillations.
- Strong dependence on **chromaticity**  $\xi$ , synchrotron tune, and transverse impedance.

A simplified threshold criterion [54] for the onset of head–tail instability is:

$$|\xi| < \left| \frac{Z_{\perp}}{n} \right| \cdot \frac{I_b R}{E_0 I \nu_s},\tag{5-1}$$

where:

- ξ: Chromaticity;
- *I<sub>b</sub>*: Bunch current;
- v<sub>s</sub>: Synchrotron tune;
- *R*: Average ring radius.

Mitigation strategies include setting **positive chromaticity**, using **bunch-by-bunch feedback systems**, and minimizing broadband transverse impedance.

### 5.3. Coupled-Bunch Instabilities

In multi-bunch operation, long-range wake fields – especially those associated with **high-Q** resonant **modes** – can drive coupled oscillations of different bunches. These are known as **coupled-bunch instabilities** (CBIs).

Coupled-bunch instabilities occur when long-range fields (e.g., cavity HOMs) cause coherent oscillations across multiple bunches, often with exponential growth in amplitude.

The mode spectrum consists of M modes (for M bunches), labeled by mode number  $\mu$ . The **growth rate** for each mode is given (under rigid-bunch approximation) by:

$$\frac{1}{\tau_{\mu}} = \frac{eI_0}{2E_0T_0} \cdot Re[Z_{\perp}(\omega_{\mu})], \tag{5-2}$$

where  $\omega_{\mu}=\omega_0(pM+\mu)$  [4], [19].

High-Q modes (e.g., from RF cavities or undamped kickers) can remain resonant with a particular mode and cause large growth unless:

- The mode is **detuned** (e.g., HOM frequency shifted away).
- **HOM dampers** are installed.
- Bunch-by-bunch feedback is applied.

### 5.4. Transverse Mode Coupling Instability (TMCI)

TMCI is a single-bunch instability caused by transverse wake fields that couple different head-tail modes within the bunch. As beam current increases, two modes approach and merge, causing exponential growth [54].

Transverse mode coupling instability (also called strong head—tail instability) occurs when internal oscillation modes of the bunch hybridize due to wake fields, leading to an unstable eigenmode.

It occurs even at zero chromaticity and does not require multi-bunch interactions. The threshold current for TMCI depends on:

- Bunch length.
- Wake function shape and amplitude.
- Transverse impedance.

Mitigation strategies include:

- Minimizing broadband transverse impedance.
- Increasing bunch length (e.g., with harmonic cavities).
- Applying active feedback.

### 5.5. Growth Rates and Damping Mechanisms

The instability **growth rate**  $1/\tau$  is often compared to the natural **radiation damping time** or to the response time of feedback systems [19].

The growth rate  $1/\tau$  characterizes how quickly a perturbation grows due to an instability. If this rate exceeds damping or feedback response, instability develops.

To suppress instabilities:

- Radiation damping (inherent in storage rings) can help stabilize low-current beams.
- Landau damping: arises from spread in betatron or synchrotron frequencies (due to nonlinear fields), providing phase mixing.
- Feedback systems: detect and correct oscillations in real time [55].

In high-current light sources, **bunch-by-bunch feedback** is essential. Modern digital systems can damp both longitudinal and transverse CBIs across hundreds of bunches.

#### 5.6. Summary of Stability Criteria

The stability of stored beams in synchrotron light sources is governed by various impedance-driven instabilities, each sensitive to specific machine parameters and beam conditions. Understanding the dominant impedance sources and key instability drivers enables the application of appropriate mitigation strategies. The Table 4 below summarizes the main types of instabilities encountered, the impedance characteristics that drive them, the critical parameters involved, and the standard approaches used to maintain beam stability.

Table 4 Overview of Instability Mechanisms and Mitigation Strategies

<b>Instability Type</b>	Dominant Impedance	Key Parameters	Typical Mitigation
Head-Tail	Transverse broadband	Chromaticity, wake slope	Positive ξ, feedback
(single-bunch)	Transverse broadband	Cinomaticity, wake slope	
TMCI	Transverse broadband	Wake amplitude, bunch length	Bunch lengthening,
TIVICI	Transverse broadband	wake ampilitude, bullen length	feedback
Mionovyovo (CD)	I an aits dinal base dhan d	7./2 8	Harmonic cavities,
Microwave (SB)	Longitudinal broadband	$Z_{\parallel}/n, \delta$	damping
Coupled-Bunch	Longitudinal or transverse	HOM frequency, Q, mode number	HOM dampers,
(multi-bunch)	narrowband	110W frequency, Q, friede flumber	detuning, feedback

### 6. Summary

Impedance plays a central role in defining the stability and performance limits of synchrotron light sources. As beam currents rise and bunch lengths shorten, collective effects driven by impedance – such as energy loss, tune shifts, and instabilities – become increasingly significant.

Understanding and mitigating both longitudinal and transverse instabilities requires a combination of theoretical tools (e.g., impedance models, instability thresholds) and practical solutions such as feedback systems, harmonic cavities, and low-impedance vacuum components.

Effective impedance control is essential for ensuring stable, high-brightness operation in modern and nextgeneration light sources.

#### 7. References

[1] W.K.H. Panofsky and W.A. Wenzel, "Some Considerations Concerning the Transverse Deflection of Charged Particles in Radio-Frequency Fields," Review of Scientific Instruments, **27**, 967 (1956).

DOI: 10.1063/1.1715427

- [2] V.G. Vaccaro, Longitudinal Instability of a Coasting Beam above Transition, Part I: Zero Coupling Impedance, CERN ISR-RF/66-35 (1966).
- [3] E. Keil and W. Schnell, *Concerning longitudinal stability in the ISR*, CERN-ISR-TH-RF-69-48, CERN, Geneva, 1969.
- [4] A.W. Chao, Physics of Collective Beam Instabilities in High Energy Accelerators, John Wiley & Sons, 1993. ISBN: 978-0-471-55184-3
- [5] T. Weiland, M. Timm and I. Munteanu, "A practical guide to 3-D simulation," IEEE Microwave Magazine, vol. 9, no. 6, pp. 62-75, December 2008, DOI:10.1109/MMM.2008.929772.
- [6] K.L.F. Bane, & M. Sands, (1985). Wakefields of Very Short Bunches in an Accelerating Cavity. SLAC-PUB-4441.
- [7] F.J. Sacherer, "Transverse bunched beam instabilities theory", in Proceedings of the 1974 CERN Accelerator School, Conf. Proc. C 740502, pp. 347–351 (1975), CERN-MPS-INT-BR-74-8.

- [8] K. Yokoya, "Impedance of slowly tapering structures", Particle Accelerators, vol. 41, pp. 221–248, 1993.KEK Preprint 93-196.
- [9] K. Yokoya, Resistive wall impedance of beam pipes of general cross section, CERN-SL-90-88-AP, CERN, 1990.
- [10] M. Izawa, S. Tokumoto, S. Sakanaka, and H. Kobayakawa, "Higher-Order-Mode Damping Coupler for Beam Instability Suppression," Japanese Journal of Applied Physics, vol. 26, no. 10R, p. 1733, Oct. 1987, DOI: 10.1143/jjap.26.1733.
- [11] H. Kobayakawa, M. Izawa, S. Sakanaka, S. Tokumoto, "Suppression of beam instabilities induced by accelerating cavities", Rev. Sci. Instrum. 1 July 1989; 60 (7), pp. 1732–1735.
  DOI: https://doi.org/10.1063/1.1140941
- [12] M. Izawa, T. Kiuchi, S. Tokumoto, Y. Hori, S. Sakanaka, M. Kobayashi, H. Kobayakawa, "Impedance measurements at the Photon Factory storage ring," Rev. Sci. Instrum. 1 January 1992; 63 (1), pp. 363–366. https://doi.org/10.1063/1.1142756 2.
- [13] S. Sakanaka, T. Mitsuhashi and T. Obina, "Measurement of quadrupolar tune shifts after the reconstruction of the Photon Factory storage ring," 2007 IEEE Particle Accelerator Conference (PAC), Albuquerque, NM, USA, 2007, pp. 4039-4041, DOI: 10.1109/PAC.2007.4439956.
- [14] S. Sakanaka, T. Mitsuhashi and T. Obina "Observation of transverse quadrupolar tune shifts in the Photon Factory storage ring," Phys. Rev. ST Accel. Beams 8, 042801 DOI:
  - https://doi.org/10.1103/PhysRevSTAB.8.042801
- [15] N. Nakamura, S. Sakanaka, K. Haga, M. Izawa and T. Katsura, "Collective effects in single bunch mode at the Photon factory storage ring," Conference Record of the 1991 IEEE Particle Accelerator Conference, San Francisco, CA, USA, 1991, pp. 440-442 vol.1, DOI: 10.1109/PAC.1991.164327.
- [16] Y.H. Chin, "Wake, impedance and instabilities," OHO'96 textbook, Vol. VI (1996) pp. 1-26.
- [17] Y.H. Chin, "Impedance and wakefield," OHO'99 textbook, Vol. 2C (1999) pp. 1-15.
- [18] Y. Shobuda and Y.H. Chin, "Impedance, wakefield and loss factor," OHO'11 textbook, Vol. 2 (2011) pp. 1-24.
- [19] K.Y. Ng, (2006). *Physics of Intensity Dependent Beam Instabilities*. World Scientific.
- [20] R. Wanzenberg, *Impedances and Instabilities*, Lecture Notes in Physics 400, in "Wake fields and

- impedances," pp. 39–79, edited by T. Weiland et al., Springer-Verlag, 1992; also presented at the CERN–CAS Winter School (Glumslöv, Sweden), June 2017.
- [21] V. Smaluk et al., "Coupling impedance of an invacuum undulator: Measurement, simulation, and analytical estimation.," Phys. Rev. ST Accel. Beams, vol. 17, p. 074402, Jul. 2014.
- [22] A. Piwinski., "Impedance in lossy elliptical vacuum chambers," DESY, Hamburg, Germany, Report No. DESY-94- 068, Apr. 1994.
- [23] O. Frasciello and M. Zobov, *Numerical Calculations* of Wake Fields and Impedances of LHC Collimators' Real Structures, arXiv:1511.01236 [physics.acc-ph], 2015.
- [24] C. Zannini et al., *Electromagnetic Simulations of Wake Fields and Impedances of LHC Collimators*, CERN Yellow Report CERN-2017-003, 2017.
- [25] O. Tanaka, N. Nakamura, T. Obina, K. Tsuchiya, R. Takai, S. Sakanaka, N. Yamamoto, R. Kato, and M. Adachi, *Impedance Evaluation of the PF In-Vacuum Undulator: Theory, Simulations, and Measurements*, in *J. Phys.: Conf. Ser.*, vol. 1067, 6, 062008 (2018). doi:10.1088/1742-6596/1067/6/062008
- [26] B. Bian, N. Yamamoto, N. Nakamura, O. Tanaka, Y. Tanimoto, T. Honda & T. Obina, Impedance Benchmarking of Resistive Wall and Tapered Transitions for the PF-HLS, Paper WEPM078, in Proceedings of IPAC'25 (International Particle Accelerator Conference), May–June 2025, pp. 2110.
- [27] R. Wanzenberg, (2003). *Impedances and Instabilities*. TESLA Report 2001-33, DESY.
- [28] Dassault Systèmes, CST Studio Suite Particle Studio, Version 2025, .

  <a href="https://www.3ds.com/products-services/simulia/products/cst-studio-suite/">https://www.3ds.com/products-services/simulia/products/cst-studio-suite/</a>
- [29] I. Zagorodnov, K. L. F. Bane & G. Stupakov, Calculations of Wakefields in 2D Rectangular Structures, Phys. Rev. ST Accel. Beams, 18, 104401 (2015).
- [30] I. Zagorodnov and T. Weiland, *The Short-Range Transverse Wake Function for TESLA Accelerating Structure*, DESY-TESLA-03-23, 2003.
- [31] T. Liebig, openEMS Open Electromagnetic Field Solver, General and Theoretical Electrical Engineering (ATE), University of Duisburg–Essen, 2010–2023; available at <a href="https://www.openEMS.de">https://www.openEMS.de</a>.
- [32] Y. H. Chin, *ABCI: Azimuthal Beam Cavity Interaction code*, KEK, 1991–present.
- [33] T. Weiland, TBCI—New Computer Code for Wake Field and Cavity Mode Calculations, in Proceedings

- of the 1983 IEEE Particle Accelerator Conference (PAC'83), Denver, CO, USA, pp. 2489–2491 (1983).
- [34] ANSYS, Inc., ANSYS HFSS (High-Frequency Structure Simulator) Electromagnetic Field Simulation, Version 2025 R1, ANSYS, Inc., 2025; available at www.ansys.com.
- [35] L. Xiao, L. Ge, Z. Li, C.-K. Ng et al., "Advances in Parallel Finite Element Code Suite ACE3P," *Proc. LINAC'10 / IPAC'10 / ABP-RF Seminar*, . SLAC-PUB-14349, 2010.
- [36] R. Gluckstern, G. Weintritt, R. Arnold, et al., *MAFIA Solution of Electromagnetic Field Problems by the Finite Integration Program*, *IEEE Trans. Microw. Theory Tech.*, vol. 39, no. 6, pp. 746–752, Jun. 1991.
- [37] L.-Q. Lee, Z. Li, C. Ng, K. Ko, Omega3P: A Parallel Finite-Element Eigenmode Analysis Code for Accelerator Cavities, SLAC-PUB-13529 (2009).
- [38] K. Halbach and R. Holsinger, .

  \*POISSON/SUPERFISH Group Codes\*, Los Alamos
  National Laboratory, 1987–present.
- [39] U. van Rienen and T. Weiland, Cavity and Waveguide Design by Triangular Mesh Code URMEL-T, in Proceedings of the 1986 Linear Accelerator Conference (LINAC'86), SLAC-Report-303, pp. 16–18, 1986.
- [40] CERN, *LHC Impedance Database*, available at <a href="https://lhc-impedance.web.cern.ch/">https://lhc-impedance.web.cern.ch/</a>
- [41] Brazilian Synchrotron Light Laboratory (LNLS). (2017). Evaluation and attenuation of Sirius components impedance. In Proceedings of IPAC 2017.
- [42] G. Skripka, (2015). *Impedance and instabilities in the MAX IV 3 GeV ring*. MAX IV Laboratory, Lund University.
- [43] A. D'Elia, J. Jacob, V. Serrière, & X. Zhu, (2021). Design of 4th harmonic RF cavities for ESRF-EBS. In Proceedings of the 12th International Particle Accelerator Conference (IPAC 2021).
- [44] D.Wang, J.M. Byrd, S. De Santis, & D. Robin, (2021). The broad-band impedance budget in the storage ring of the ALS-U project. In Proceedings of the 12th International Particle Accelerator Conference (IPAC'21), Campinas, SP, Brazil, pp. 204–207.
  - DOI: 10.18429/JACoW-IPAC2021-MOPAB359.
- [45] R. Nagaoka, & K.L.F. Bane, (2014). *Collective effects in a diffraction-limited storage ring*. In Journal of Synchrotron Radiation, 21, 937–960. DOI: 10.1107/S1600577514015215.
- [46] R. Nagaoka, (2005). *Numerical evaluation of geometric impedance for SOLEIL*. In Proceedings of

- the Particle Accelerator Conference (PAC'05), Knoxville, TN, USA, pp. 2654–2656.
- [47] European Synchrotron Radiation Facility (ESRF). (2019). EBS storage ring technical design report. ESRF Design Report (Phase II Upgrade).
- [48] S. Khan, (1998). Beam impedance study for the BESSY II storage ring. In Proceedings of the 1997 Particle Accelerator Conference (PAC'97), Vancouver, Canada, pp. 2627–2629. (CERN AccelerConf archive: pac97/papers/pdf/7V027.PDF)
- [49] B. Zotter, & S. Kheifets, (1998). *Impedances and Wakes in High-Energy Particle Accelerators*. World Scientific.
- [50] R. L. Warnock, (1994). Coherent synchrotron radiation and bunch lengthening in electron storage rings. Nuclear Instruments and Methods in Physics Research Section A, 347(1-3), 113–117.
- [51] K.L.F. Bane, & B.W. Zotter, (1990). *Impedances of small discontinuities for round and flat chambers*. Particle Accelerators, 25, 113–137.
- [52] E. Keil, & W. Schnell, (1969). Collective Instabilities and High Frequency Resistive Wall Effects in Proton Storage Rings. CERN Report, CERN 69-15.
- [53] D. Boussard, (1983). Observation of microwave longitudinal instability in the CPS proton storage ring. IEEE Transactions on Nuclear Science, 30(4), 2241–2243.
- [54] F.J. Sacherer, (1977). *Transverse bunched beam instabilities theory*. IEEE Transactions on Nuclear Science, 24(3), 1393–1399.
- [55] D. Teytelman, J. Fox, H. Hindi, & D. Sagan, (2005). Measurements and Modeling of Coupled Bunch Instabilities at the ALS. Proceedings of the 2005 Particle Accelerator Conference (PAC), Knoxville, TN, USA, 2005, pp. 2810–2812.